PERGAMON

International Journal of Heat and Mass Transfer 44 (2001) 645–657

International Journal of HEAT and MASS TRANSFER

www.elsevier.com/locate/ijhmt

Laser-based thermal pulse measurement of liquid thermophysical properties

J. Sun, J.P. Longtin*, T.F. Irvine Jr

Department of Mechanical Engineering, State University of New York at Stony Brook, Stony Brook, NY 11794-2300, USA

Received 18 October 1999; received in revised form 8 March 2000

Abstract

In this work, a laser-based thermal pulse technique is presented that simultaneously measures thermal conductivity and thermal diffusivity for liquids, from which the volumetric specific heat can be determined as well. The measurement is based on photothermal deflection of a HeNe laser beam that passes through the test liquid next to a thin heating wire. Liquid thermophysical properties are determined by fitting a numerical simulation of the heat conduction and probe beam deflection to the measured time-dependent probe beam deflection. Results are presented for five liquids: glycerol, 1-propanol, 2-propanol, methanol, and ethanol, and are found to be in very good agreement with values reported in the literature. The experimental setup is small, inexpensive and reliable. The temperature dependence of the liquid refractive index is also determined during the measurement process, and the same experimental technique is capable of measuring the thermal conductivity and thermal diffusivity of thin conducting wires.

1. Introduction

The accurate measurement of thermal conductivity k and thermal diffusivity α for liquids is vital not only for practical engineering, but also for theoretical studies and analyses. Being transport properties, the thermal conductivity and thermal diffusivity are more difficult to measure than thermodynamic properties such as density and specific heat. In many conventional measurements, the transport equations were used directly by measuring heat flux and/or temperature gradients [1], both of which are difficult to measure. Heat losses at the boundaries, convection, and radiation in the test liquids were significant error sources. In addition, only one property was measured, e.g. k or α, as these techniques were not able to simultaneously determine both liquid thermal conductivity and thermal diffusivity.

The transient hot-wire technique, which is typical among the conventional methods, has been widely used to measure liquid thermal conductivity or thermal diffusivity [2–5]. A wire immersed in the test liquid is electrically heated. The liquid thermal conductivity and thermal diffusivity are determined by measuring the temperature variation history of the wire, which depends on the liquid thermophysical properties. One major difficulty with the hot-wire technique is natural convection, which occurs due to buoyancy effect from prolonged heating of the wire.

The unique properties and non-invasive nature of laser light have made it an attractive measurement tool. Examples include laser flash methods [6,7], laser-induced thermal grating [8–10], thermal lensing

* Corresponding author. Tel.: +1-631-6329436; fax: +1-631-6328544.

E-mail address: jlongtin@ms.cc.sunysb.edu (J.P. Longtin).

0017-9310/01/$ - see front matter
PII: S0017-9310(00)00119-8

Nomenclature

a	heating wire radius (m)
C_p	specific heat (J/kg K)
d	distance between probe laser beam and heating wire centerline (m)
I	current (A)
k	thermal conductivity (W/m K)
L	probe laser beam path length in air (m)
l	heating wire length (m)
n	refractive index
$\dot{Q}'''$	volumetric heat generation rate in heating wire (W/m^3)
r	radial direction (m)
T	transmissivity; temperature (°C, K)
t	time (s)
V	heating voltage (V); position-to-voltage converter output voltage (V)
W	probe laser beam path length in liquid (m)
w	half width of glass cell (m)
x	spatial direction perpendicular to probe laser beam (m)
$\vec{x}$	spatial unit vector in direction perpendicular to probe laser beam
z	spatial direction parallel to probe laser beam (m)

Greek symbols

α	thermal diffusivity (m^2/s)
δ	probe laser beam displacement on position detector (m)
ε	total error between normalized model and experimental data (V^2/J^2)
θ	probe laser beam deflection angle (rad)
ρ	density (kg/m^3)
φ	azimuthal angle (rad)

Subscripts

0	initial condition
air	air
e	experiment
f	liquid
j	dummy index
m	model
p	pulse
w	wire
δ	probe laser beam deflection
∞	far field

techniques [11], and holographic interferometry [12], among others. In some cases, good results have been reported by these techniques, however, they suffer from one or more of the following shortcomings: unavoidable measurement deviation due to heat losses into the test liquid, a complicated experimental setup, difficult optical alignment, and/or a strong dependence on the accuracy of interferometry fringes. In addition, only one liquid property can be determined, which is a common disadvantage of all these methods.

A technique related to the present work was reported by Kim and Irvine [13], in which the thermophysical properties of non-Newtonian liquids were determined using a thermal pulse technique. The time for thermal energy from a multilayer heating element to travel a known distance between two points in the liquid was measured by monitoring temperature peaks at the two points using thermocouples. However, this technique is limited by the finite size of the thermocouple, which causes uncertainties in the temperature measured at the two points. In the present work, photothermal deflection [14] is combined with the thermal pulse technique to simultaneously measure liquid thermal conductivity and thermal diffusivity, where a non-invasive laser beam is used as the probe. Although photothermal deflection has been employed to measure the thermal diffusivity of solids [15,16] and gases [17], very limited investigations have been reported for liquids [18].

A CW HeNe laser probe beam is sent through the test liquid next to a thin, circular nickel–chromium (NiCr)-alloy wire immersed in the liquid serving as a heating source. During a square heating pulse, a temperature gradient is formed in the liquid, which, in turn, causes a gradient in the liquid refractive index, due to which the probe laser beam is deflected from its nominal position on a position detector. The test liquid needs only to have a moderate transmission $T \geq 0.01$ for enough laser light to pass through it to strike the detector. The time-varying beam deflection is recorded and compared with a numerical model, in which the liquid thermal conductivity and thermal diffusivity are adjusted and determined to yield the best agreement. Results are presented for five liquids: glycerol, 1-propanol, 2-propanol, methanol, and ethanol, and are found to be in good agreement with the values found in the literature. Since $\alpha = k/\rho C_p$, the volumetric specific heat ρC_p can also be determined. The experimental setup is small, inexpensive and reliable. Additionally, the tem-

perature dependence of the liquid refractive index, dn/dT, is determined during the measurement process.

2. Experimental setup and theory

2.1. Experimental setup

The experimental configuration is shown in Fig. 1. A Melles-Griot 1 mW HeNe CW laser with a wavelength of 632.8 nm serves as the probe beam source. The test liquid resides in a square glass cell with interior dimensions of 50 × 50 × 50 mm. After being focused by a singlet lens with a focal length of 50 mm, the beam passes through the test liquid, exits, and strikes a UDT LSC-5D semiconductor position detector, by which the beam displacement can be measured. A calibrated small thermistor immersed in the test liquid measures the liquid temperature with an uncertainty of less than 0.05°C.

A NiCr alloy resistance wire with length l = 22 mm is completely immersed in the test liquid as the heating source. Since the wire is completely immersed several millimeters below the liquid surface, there is no surface effect. The NiCr wire is homogeneous, resulting in uniform heat generation in the wire. However, the wire is not isothermal since the heat generated is conducted radially to the wire surface. The wire diameter was measured using a diffraction technique [19], and was found to be 258 ± 2 μm; the wire resistance was measured using a precision multimeter and found to be 2.38 ± 0.05 Ω/cm. The wire is oriented vertically and perpendicular to the probe beam. As discussed later, this setup minimizes natural convection effects when configuring the system. The wire is mounted on a translation stage so that it can be positioned with respect to the probe beam. A dial indicator with 1-μm

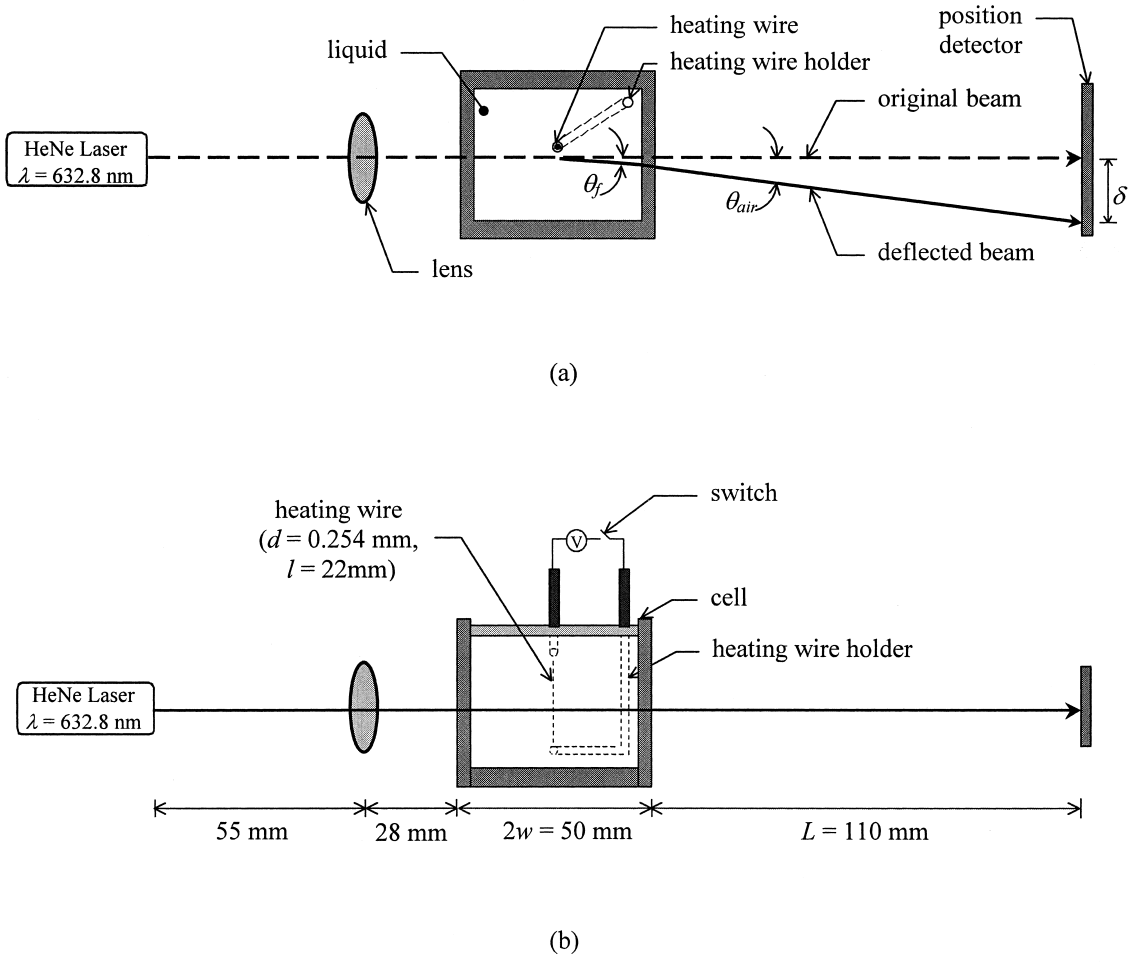

Fig. 1. Experimental setup and optical path (a) top view; (b) side view.

resolution is used to monitor the wire position. In this work the wire is used only as a heating source and not as a sensing element as is the case with the hot-wire technique [2–5]. It is thus not necessary to measure the wire temperature during the experiment.

A timing circuit controls the heating current through the wire during the heating pulse, which is supplied by a dc power supply. A single heating pulse is used, with a typical duration of 0.3 s, and with a heating voltage ranging from 0.2 to 0.5 V. The heating wire voltage and current are measured using two Keithley Model 2000 multimeters.

Heat generated in the wire is conducted into the liquid, causing a time- and position-dependent temperature gradient, which causes the probe beam to deflect from its nominal position on the position detector. The detector output current is sent to a position-to-voltage converter, which produces an output voltage linearly proportional to the beam position. The measured detector/amplifier sensitivity is 2.72 ± 0.03 mV for a 1-μm displacement on the detector. Both the heating pulse voltage and the position sensor output are recorded with a Tektronix TDS 380 two-channel digitizing oscilloscope.

The position-to-voltage converter also provides a voltage that is linearly proportional to the absolute intensity of the probe laser beam incident on the position detector, regardless of its position. This feature allows the position detector to be used as a light meter, and is employed in the determination of the distance between the probe laser beam and the wire discussed below.

2.2. Photothermal deflection model

An analytical expression for the beam deflection angle in the liquid, θ_f (Fig. 1a), can be expressed as [20]:

$$\theta_f = \int_0^W \frac{\nabla n \cdot \vec{x}}{n} \, dz \cong \frac{1}{n_0} \int_0^W (\nabla n \cdot \vec{x}) dz \tag{1}$$

where n is the refractive index of the liquid, W is the probe beam path length in the liquid, and $\vec{x}$ is the spatial unit vector in the direction perpendicular to the probe beam, respectively. Since the normalized change in the liquid refractive index, $\Delta n/n$, is of the order of 10^{-3} or less, the refractive index can be approximated as a nominal value n_0, and taken out of the integral in Eq. (1). The refractive index gradient is related to the temperature gradient by

$$\nabla n = \frac{dn}{dT} \nabla T, \tag{2}$$

where dn/dT is the change in refractive index with temperature. In this experiment, the maximum liquid temperature increase is $<4^\circ$C (see below), hence dn/dT can be taken as a constant, and also removed from the integral in Eq. (1). Therefore, Eq. (1) can be rewritten as

$$\theta_f = \frac{1}{n_0} \frac{dn}{dT} \int_0^W (\nabla T \cdot \vec{x}) dz. \tag{3}$$

Referring to the wire and probe beam geometry in Fig. 2,

$$\nabla T \cdot \vec{x} = \frac{dT}{dx} = \cos\varphi \frac{dT}{dr} = \frac{d}{(d^2 + z^2)^{1/2}} \frac{dT}{dr}, \tag{4}$$

Eq. (3) then becomes

$$\theta_f = \frac{1}{n_0} \frac{dn}{dT} \int_{-w}^{w} \frac{d}{(d^2 + z^2)^{1/2}} \frac{dT}{dr} dz, \tag{5}$$

where d is the distance between the probe beam and the wire centerline, and w is the half width of the glass cell, respectively. Eq. (5) represents the beam deflection angle in the liquid, and its dependence on the temperature gradient dT/dr, which varies with both position and time. Snell's law is used to relate the beam deflection angle in the air with that in the liquid:

$$\theta_{air} = \theta_f \frac{n_0}{n_{air}} \cong n_0 \theta_f, \tag{6}$$

where the air refractive index, $n_{air} \approx 1.0$, and $\sin\theta \approx \theta$ since the beam deflection angle is small. The angle shown in Fig. 1a is greatly exaggerated.

2.3. Thermal model

Liquid thermal conductivity k_f and thermal diffusivity α_f are determined by observing their influence on a measurable quantity, namely the probe beam deflection; as such, this measurement is an *inverse problem*. A thermal model for the heat conduction with guess values of k_f and α_f is solved for the temperature gradient dT/dr within the test liquid, from which the time-dependent probe beam deflection can be calculated using Eqs. (5) and (6).

Since the aspect ratio of wire diameter to length, $2a/l \sim 0.01$, end effects in the wire can be neglected, and the heat conduction can be considered to be in the radial direction only. Also, the experiment is completed in less than 0.5 s, during which time the thermal energy diffuses only ~1 mm, hence the liquid, which resides in a 50-mm container, can be approximated as an infinite medium. Furthermore, due to liquid inertia, it will take some time for natural convection to come into effect after the start of the heating pulse. Since the time scale of the measurement is <1 s, and the tem-

perature rise in the wire is small (see below), natural convection is ignored.

Using cylindrical coordinates, the governing equations for heat conduction in the wire and the liquid are, respectively,

$$\frac{1}{\alpha_w}\frac{\partial T_w}{\partial t} = \left(\frac{\partial^2 T_w}{\partial r^2} + \frac{1}{r}\frac{\partial T_w}{\partial r}\right) + \frac{\dot{Q}'''}{k_w} \tag{7a}$$

and

$$\frac{1}{\alpha_f}\frac{\partial T_f}{\partial t} = \frac{\partial^2 T_f}{\partial r^2} + \frac{1}{r}\frac{\partial T_f}{\partial r} \tag{7b}$$

with boundary conditions

$$\left.\frac{\partial T_w}{\partial r}\right|_{r=0} = 0 \tag{8a}$$

$$-k_w \left.\frac{\partial T_w}{\partial r}\right|_{r=a} = -k_f \left.\frac{\partial T_f}{\partial r}\right|_{r=a} \tag{8b}$$

$$T_w|_{r=a} = T_f|_{r=a} \tag{8c}$$

$$T_f|_{r\to\infty} \to T_\infty \tag{8d}$$

and initial conditions

$$T_w|_{t=0} = T_f|_{t=0} = T_\infty \tag{9a}$$

$$\dot{Q}''' = \begin{cases} VI/\pi a^2 l & 0 \le t \le t_p \\ 0 & t > t_p \end{cases} \tag{9b}$$

where a is the radius of the wire, t_p is the time duration of the heating pulse, $\dot{Q}'''$ is the volumetric heat generation rate in the wire, V and I are the heating wire voltage and current, and the subscripts w and f refer to wire and liquid, respectively.

2.4. Numerical simulation

Although Carslaw and Jaeger [21] have discussed the analytical solution to a heat conduction problem similar to Eqs. (7a), (7b), (8a), (8b), (8c), (8d), (9a) and (9b) using Laplace transforms, the solution, unfortunately, is in the form of an indefinite integral containing Bessel functions in a nontrivial form, and cannot be readily introduced into Eq. (5) to solve for the probe beam deflection. Therefore, Eqs. (5), (6), (7a),

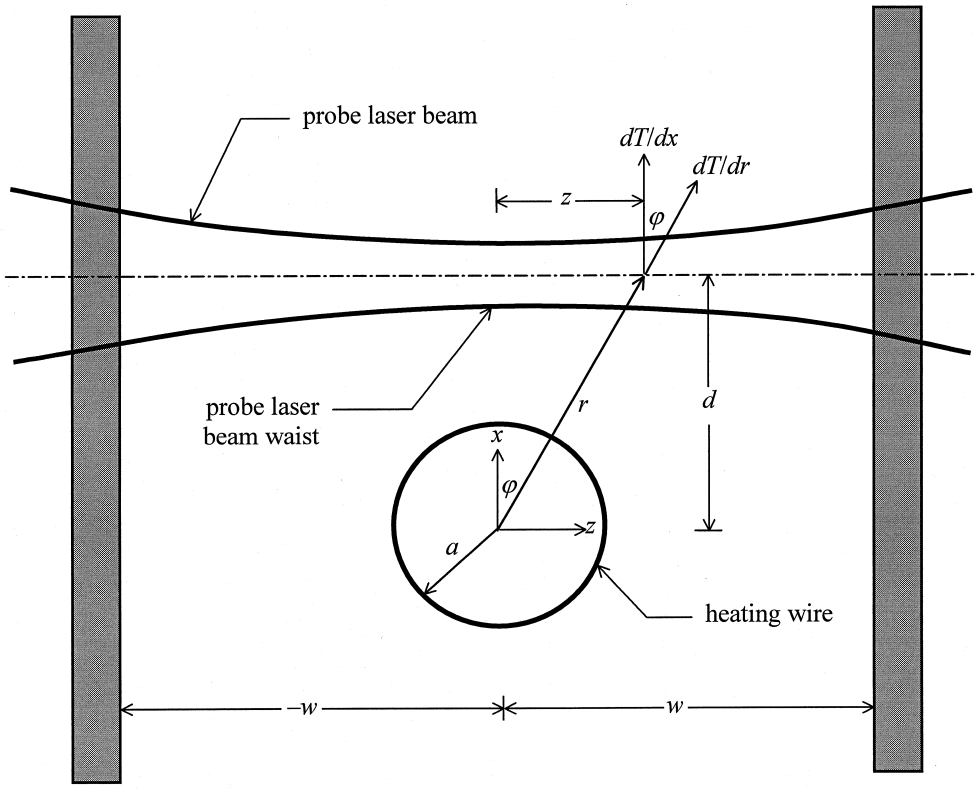

Fig. 2. Geometry of heating wire and probe laser beam. Variation in probe laser beam diameter greatly exaggerated.

(7b), (8a), (8b), (8c), (8d), (9a) and (9b) are solved numerically with an explicit finite difference scheme to determine the temperature gradient and the beam deflection. Using a node-centered grid, the spatial derivatives in Eqs. (7a) and (7b) are discretized by a second-order-accurate central differencing scheme, and the temporal derivative is approximated as a first order forward difference in time.

The liquid thermal conductivity k_f, and thermal diffusivity α_f, appear in Eqs. (7b) and (8b) as unknown parameters. Temperature gradients solved with different values of k_f and α_f through the numerical simulation will differ from each other, and thus results in different time-dependent beam deflection in Eq. (5). Therefore, k_f and α_f can be determined by searching for those values that yield the best agreement between the probe beam deflection from the numerical model and that recorded during the experiment.

2.5. System calibration

There are two additional unknown parameters in Eqs. (7a) and (8b): the wire thermal conductivity k_w and thermal diffusivity α_w. The values of k_w and α_w are difficult to measure directly, however, they can be determined by using a liquid with known values of k_f and α_f in the existing experimental setup. The experimental procedure is identical, except that the unknowns become k_w and α_w. Due to its well-studied properties, water is used as the calibration liquid, and results in measured values of $k_w = 10.31$ W/m K and $\alpha_w = 1.86 \times 10^{-6}$ m^2/s. In fact, the same experimental technique can be used as a general-purpose measurement for thermal conductivity and thermal diffusivity of thin conducting wires.

3. Results and discussion

3.1. Effects of finite probe beam diameter

Since the nominal beam exiting the laser has a diameter of ~0.7 mm, a singlet lens with a focal length of 50 mm is used to focus the probe laser beam down to a waist to minimize the spatial variation of the beam with respect to the wire (Fig. 2). The actual beam waist size and the focal point position for each test liquid are first calculated using a matrix transformation method of geometrical optics, and then verified by measuring the beam diameter at several points in the beam path using a knife-edge technique [22]. Very good agreement between measured and predicted values are found, resulting in a beam waist of 71 ± 2 μm. After determining the beam waist, the heating wire is centered at the beam waist, as shown in Fig. 2.

In the numerical model, the probe beam is considered to be infinitely thin, which simplifies the numerical modeling, and results in significantly improved calculation times. To assess the effects of a finite-size probe beam, the numerical model for the beam deflection is modified by considering the beam cross-section to be evenly broken up into 10–20 vertical thin ribbons, parallel to the heating wire, with each ribbon at a different distance from the wire as determined by the waist diameter. The final beam deflection is then taken as the sum of the deflections of all ribbons, with the contribution from each ribbon weighted by its power determined by a Gaussian intensity distribution. The difference between the beam deflection resulting from the multi-ribbon calculation and the infinitely thin beam assumption is negligibly small, and indicates that the latter is a very good approximation to the finite beam, provided the beam diameter is smaller than the distance between the beam and the wire centerline.

3.2. Heating wire–probe beam distance

The distance between the probe laser beam and the heating wire centerline, d, in Fig. 2 is critical in Eq. (5), and it is imperative to measure this value accurately. In the experimental setup, a mechanical dial indicator graduated with 1-μm increments provides accurate relative displacements of the heating wire in the x direction. If, then, the wire–probe distance can be accurately determined at one point, the position of the wire at other points can be accurately determined as well. One position well suited for a reference point is the point where the heating wire is located directly in front of the laser beam, i.e. $d = 0$ in Fig. 2. As the wire is moved through the beam, the intensity captured by the position detector behind the wire will decrease, reach a minimum, and increase again. The light meter feature of the position detector can be used to monitor such an intensity variation as the wire is moved through the beam. The positions of the wire when the intensity is 50% of the unblocked intensity are recorded, both when the wire approaches and moves away from the beam. The midpoint of these two positions represents the candidate zero offset position, $d = 0$. The final zero offset position is determined by comparing experimental deflection curves when the probe beam is on opposite sides of the heating wire with the same offset distance, typically 300 μm. The true zero offset point is the one that makes these two experimental curves identical. In practice, the final zero point was within 3–5 μm of the candidate zero point.

3.3. Data collection and processing

Experimental probe beam deflections are recorded at two offset positions of the probe laser beam, $d = 300$ and 330 μm. The oscilloscope collects the heating wire

voltage in channel 1 and the time-dependent position sensor output voltage in channel 2. A single heating pulse is used for each scope trace. Once the scope has completed data acquisition, the data from both channels are saved in ASCII format for post-processing.

For each value of d, the experiment is repeated six to eight times, resulting in six to eight sets of data. Due to the fluctuations in the voltage and current output of the power supply, the heat generated in the wire fluctuates 2–4% from run to run. To remove this variation, the beam deflection data are normalized by dividing the original data by the heat generated in the corresponding heating pulse before they are averaged to produce the final experimental data. Comparison between the experimental data and the numerical model is then performed based on this averaged, normalized position sensor output.

To determine k_f and α_f, the probe beam deflection from the model is compared with the experimental data at every time step. The total error is then computed as

$$\varepsilon = \sum_j (V_{e,j} - V_{m,j})^2 \tag{10}$$

where $V_{e,j}$ and $V_{m,j}$ are the experimental and model values of the normalized position sensor output voltage at time j, respectively. Smaller values of ε indicate better agreement between the model and the experimental data. A search program written in Visual Basic and C then performs the comparison of various values of k_f and α_f to find those that produce the smallest ε. These values are then taken as the measured results of this experiment. The typical searching range for both k_f and α_f are $\pm 15\%$ of a guess value with a step change of 0.1%, though any range and step size can be used.

The temperature dependence of liquid refractive index, dn/dT, appears in Eq. (5) as a scale factor. The *shape* of the time-dependent probe beam deflection curve is determined by the values of k_f and α_f, while the *magnitude* is determined by dn/dT. When searching for k_f and α_f, a nominal, constant value of dn/dT is used. Since dn/dT is only a scale factor, it will not affect the best-fit values of k_f and α_f. Once these values are determined, the program searches for the value of dn/dT that provides the smallest ε in Eq. (10).

3.4. Determining k_f, α_f, and dn/dT for several liquids

Values of k_f and α_f, and dn/dT for five liquids — glycerol, 1-propanol, 2-propanol, methanol, and ethanol — have been measured. Both the normalized experimental (open circles) and numerical (solid line) probe beam deflections are shown in Figs. 3–7, where the time-dependent beam position is plotted versus time in case of $d = 300$ μm. For clarity, every sixth experimental data point is shown in the figures. The

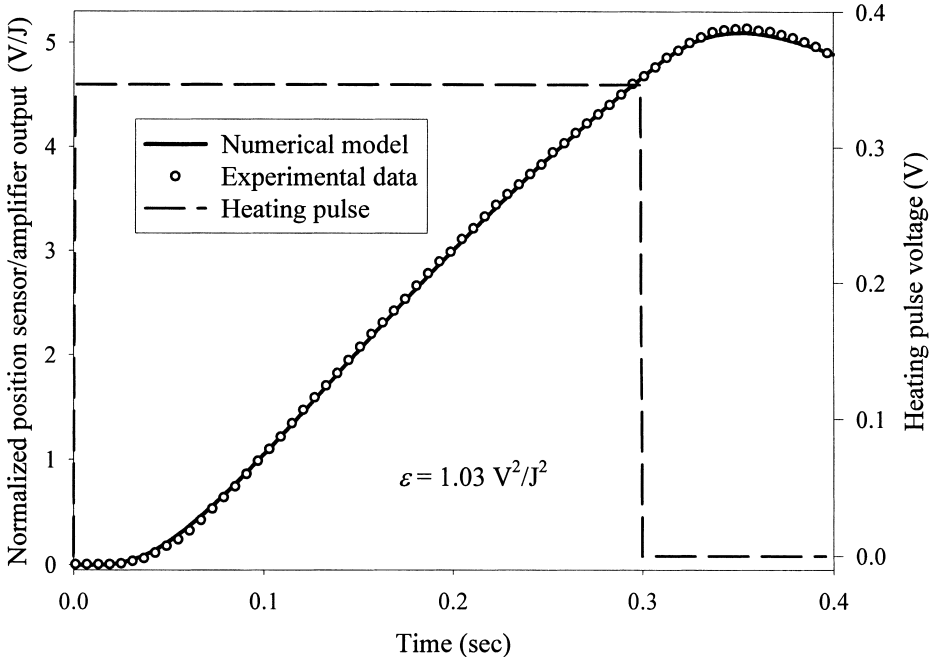

Fig. 3. Time-dependent probe beam deflection for glycerol.

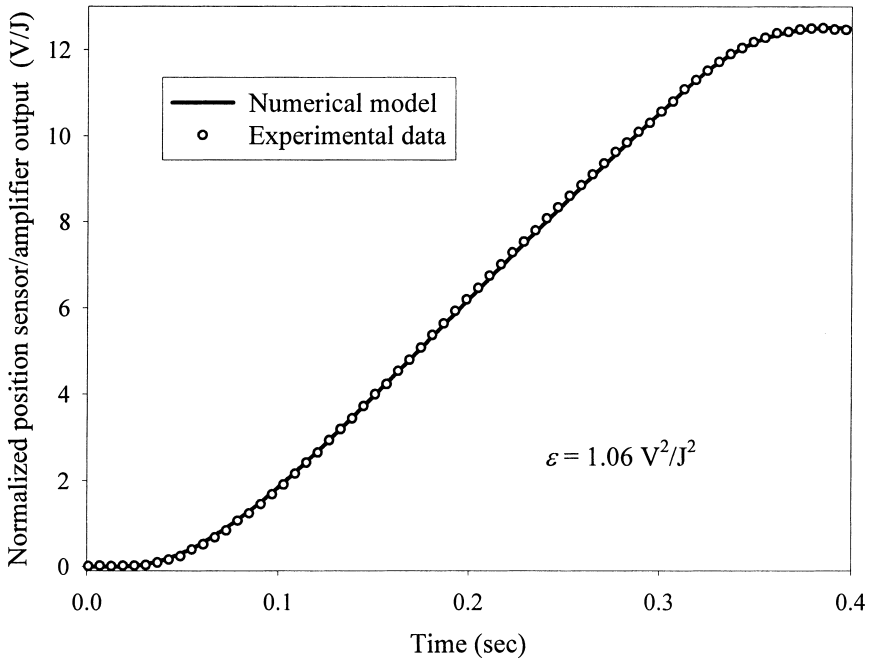

Fig. 4. Time-dependent probe beam deflection for 1-propanol.

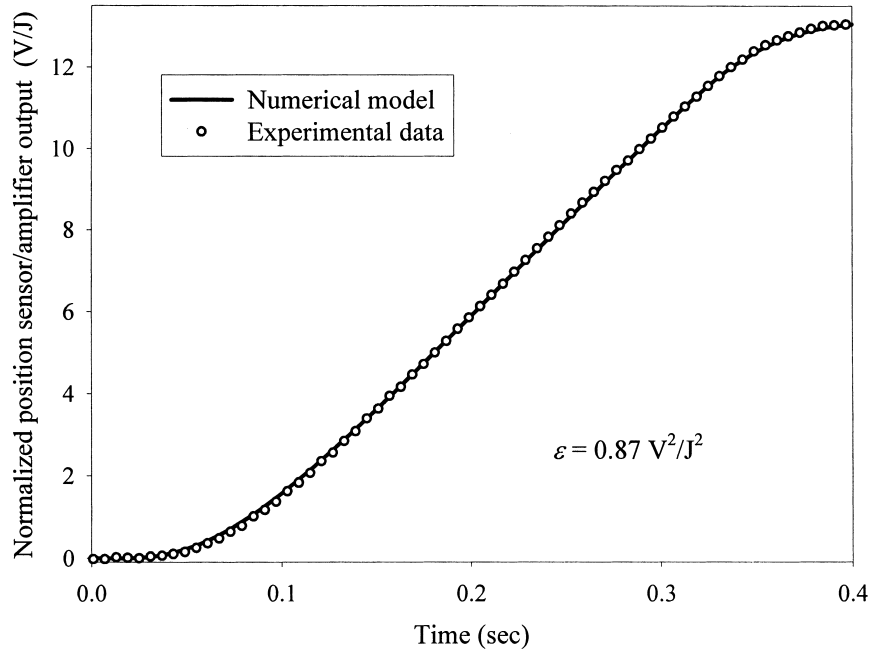

Fig. 5. Time-dependent probe beam deflection for 2-propanol.

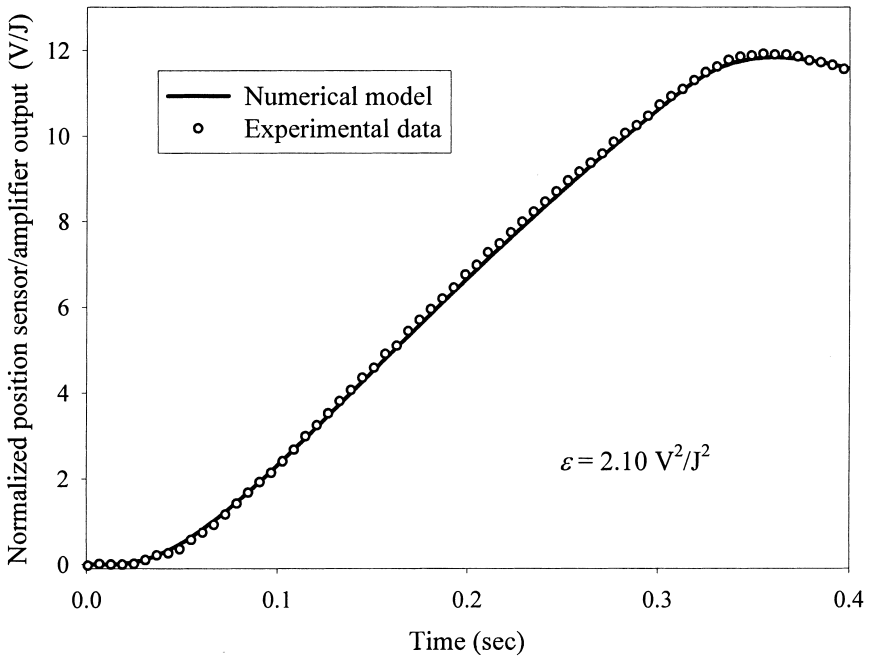

Fig. 6. Time-dependent probe beam deflection for methanol.

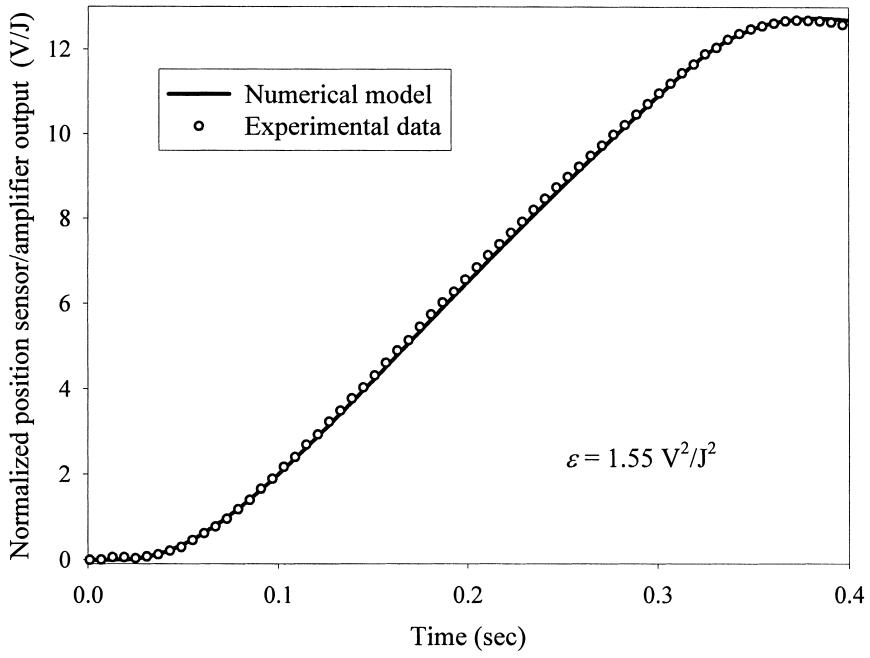

Fig. 7. Time-dependent probe beam deflection for ethanol.

heating wire voltage is also shown in the first figure (Fig. 3) to illustrate the relationship between the heating pulse duration and the probe beam deflection. Note that the agreement between the experimental and numerical results is surprisingly good, once the appropriate values of k_f and α_f, and dn/dT are selected. Though not shown here, the agreement between the model and the experimental results for $d = 330$ μm are equally good.

In all cases, features of the probe beam deflection are similar. At time $t = 0$ s, heat generation begins in the wire. Since there is a finite distance between the wire and the probe beam, however, some time is required for the thermal energy to diffuse into the path of the beam and cause deflection. The deflection increases until energy generation in the wire ceases at $t \sim 0.3$ s, and the beam deflection then reverses direction, albeit with a short time delay after the heating pulse stops. Note that the time delay between heating and probe beam deflection is comparable for both the start and the end of the heating pulse.

In deciding how much of the probe beam deflection to use in the fitting procedure, the shortest reasonable beam deflection, which starts from $t = 0$ s and includes the entire heating pulse and any time delays for the thermal energy to reach the probe beam, is chosen in this work for several reasons. First, experiments have shown that the quality and repeatability of the deflection signal degrade significantly for times after the peak signal, i.e. $t = 0.4$–0.5 s. Also, and perhaps re-

Table 1
Liquid thermal conductivity and thermal diffusivity

Test liquid	Thermal conductivity (W/m K)		Thermal diffusivity (10^{-8} m^2/s)		ε (V^2/J^2)
	Reference value	Measured value	Reference value	Measured value	
Glycerol	0.292[a] (25°C) 0.2916[b] (25°C) 0.2880[c] (26.85°C) 0.286[d] (20°C) 0.285[e] (20°C) 0.279[f] (25°C)	0.29 (23.3°C)	9.763[a] (25°C) 9.594[d] (20°C) 9.316[e] (20°C)	9.40 (23.3°C)	1.03
1-Propanol	0.172[e] (20°C) 0.157[d] (20°C) 0.1560[f] (26.85°C) 0.1553[b] (25°C) 0.154[a] (25°C)	0.16 (24.0°C)	8.811[e] (20°C) 8.327[d] (20°C) 8.034[a] (25°C)	8.05 (24.0°C)	1.06
2-Propanol	0.156[e] (20°C) 0.141[d] (20°C) 0.1400[f] (26.85°C) 0.1378[b] (25°C) 0.135[a] (25°C)	0.14 (23.2°C)	7.196[d] (20°C) 6.624[a] (25°C)	6.76 (23.2°C)	0.87
Methanol	0.212[e] (20°C) 0.2022[c] (26.85°C) 0.202[d] (20°C) 0.2011[b] (25°C) 0.2[a] (25°C) 0.2[f] (26.85°C)	0.21 (22.4°C)	10.837[e] (20°C) 10.222[d] (20°C) 10.042[a] (25°C)	10.24 (22.4°C)	2.10
Ethanol	0.182[e] (20°C) 0.173[d] (20°C) 0.1695[b] (25°C) 0.169[a] (25°C) 0.1675[f] (26.85°C) 0.1660[c] (26.85°C)	0.17 (23.5°C)	9.339[e] (20°C) 9.155[d] (20°C) 8.797[a] (25°C)	8.35 (23.5°C)	1.55

[a] Ref. [23].
[b] Ref. [24].
[c] Ref. [25].
[d] Ref. [26].
[e] Ref. [27].
[f] Ref. [28].

lated to the previous statement, shorter deflection times minimize natural convection effects, which will alter the temperature profile that the probe beam encounters.

In their measurement, which has a similar heating arrangement, Kim and Irvine [13] determined a critical Grashof number of 2×10^7 for natural convection to become important. Calculations of Grashof numbers for the five test liquids result in a maximum value of 4.1×10^5 for methanol and a minimum value of 0.15 for glycerol. As the Grashof numbers obtained for the five liquids are all much less than the critical value, natural convection effects in the present work are negligible. Note, however, that longer data collection times and/or larger temperature increases in the wire may exceed the critical Grashof number.

Both liquid thermal conductivity and thermal diffusivity are functions of temperature. During the heating pulse, the test liquid is heated by the wire, resulting in a temperature increase. To minimize temperature effects, the maximum wire temperature increase during the heating pulse is kept below 2–4°C.

Results for glycerol, 1-propanol and 2-propanol are shown in Figs. 3–5, respectively. As can be seen, the fit between numerical and experimental results is extremely good for these liquids, with low values of ε in Eq. (10) obtained (see Table 1). The results for methanol and ethanol shown in Figs. 6 and 7 are also reasonable good, however, the agreement between the numerical model and experimental data is not as good as that for the previous three liquids. Also significantly higher values of ε are obtained for methanol and ethanol, even when the best-fit values of k_f and α_f were used (Table 1). The exact nature of such a discrepancy is not clearly understood. One possible explanation is that the lower boiling point of methanol (65°C) and ethanol (78°C) [23] result in more vaporization at the liquid surface, which generates more temperature fluctuations in the liquid as a whole. In fact, an interesting observation was made when the liquid was in thermal equilibrium before the heating pulse was applied. Small beam deflections at the detector were observed due to temperature fluctuations in the liquid. The rms fluctuations for methanol and ethanol were nearly an order of magnitude greater than the other liquids. This suggests that there is more inherent fluctuation in the temperature of methanol and ethanol, which may explain the difficulty in obtaining very close fits for the results.

The final values of k_f and α_f for all the five liquids are listed in Table 1, together with several values from the literature. Note that the variation in the literature values are as high as 15%, and all measured values from this experimental technique fall within the range of values reported in the literature, with the exception of α_f for ethanol only. Measured values of dn/dT for the five test liquids are listed in Table 2, along with existing literature values. As can be seen, the agreement between the measured and literature values is also good. Since $\alpha = k/\rho C_p$, only two of these three properties are independent, hence ρC_p can be determined once k_f and α_f are known.

Table 2
Thermo-optical properties of liquids

Test liquid	n	dn/dT (10^{-4} K^{-1})	
		Reference value	Measured value
Glycerol	1.4735[a]	−2.3[b]	−2.40
1-Propanol	1.3852[a]	−3.9[c]	−4.33
	1.384[c]		
2-Propanol	1.3742[a]	−3.4[b]	−4.63
Methanol	1.329[a]	-4.68 ± 0.11[e]	−4.32
	1.325[c]	−4.28[d]	
		−3.9[c]	
Ethanol	1.3614[a]	−4.46[d]	−4.53
	1.358[c]	-4.38 ± 0.04[e]	
		−3.9[c]	

[a] Ref. [23].
[b] Ref. [29].
[c] Ref. [30].
[d] Ref. [20].
[e] Ref. [31].

3.5. Uncertainty analysis

Although liquid thermophysical properties are measured in this work, the time-dependent position-to-voltage converter output voltage, V_δ, is the actual data collected during the experiment, which is based on the measurement of a series of parameters, d, a, V, I, l and L. Due to the unavailability of an explicit relationship between V_δ and these parameters, the uncertainty in the present work is determined as follows. First, the uncertainty in V_δ is estimated by analyzing each corresponding error source; second, the uncertainties of the measured thermophysical properties are determined by running the model program to determine the effects of the uncertainty in V_δ. The final results indicate that this technique is capable of resolving both liquid thermal conductivity and thermal diffusivity of 2–3%.

4. Conclusions

Liquid thermal conductivity and thermal diffusivity are simultaneously measured using a laser-based thermal pulse technique in this work, from which the volumetric specific heat of liquid can also be determined. The experiment is based on photothermal deflection of

a laser probe beam that occurs due to a temperature gradient formed during a square heating pulse. The experimental setup is small, inexpensive and reliable. Five liquids — glycerol, 1-propanol, 2-propanol, methanol, and ethanol — were tested with good agreement found between measured and literature values, and a typical uncertainty of $\pm 2\%$ for both liquid thermal conductivity and thermal diffusivity. As an added feature, the temperature dependence of the liquid refractive index is determined during the measurement process. The technique works for transparent liquids as well as those with moderate absorption, and can be used by a new instrument to measure thermal conductivity, thermal diffusivity, volumetric specific heat, and the temperature-dependent refractive index of liquids. Alternatively, the same technique can be used to measure the thermal conductivity and thermal diffusivity of thin, conducting wires.

Acknowledgements

The authors gratefully acknowledge support for this work from the National Science Foundation under contract CTS-9702644.

References

[1] L.P. Filippov, Liquid thermal conductivity research at Moscow University, Int. J. Heat Mass Transfer 11 (1968) 331–345.
[2] Y. Nagasaka, A. Nagashima, Simultaneous measurement of the thermal conductivity and the thermal diffusivity of liquids by the transient hot-wire method, Rev. Sci. Instrum. 52 (1981) 229–232.
[3] J.D. Raal, R.L. Rijsdijk, Measurement of alcohol thermal conductivities using a relative strain-compensated hot-wire method, J. Chem. Eng. Data 26 (1981) 351–359.
[4] H. Watanabe, Accurate and simultaneous measurement of the thermal conductivity and thermal diffusivity of liquids using the transient hot-wire method, Metrologia 33 (1996) 101–115.
[5] M. Fujii, X. Zhang, N. Imaishi, S. Fujiwara, T. Sakamoto, Simultaneous measurements of thermal conductivity and thermal diffusivity of liquids under microgravity conditions, Int. J. Thermophys. 18 (1997) 327–339.
[6] Y. Tada, M. Harada, M. Tanigaki, W. Eguchi, Laser flash method for measuring thermal conductivity of liquids — application to low thermal conductivity liquids, Rev. Sci. Instrum. 49 (1978) 1305–1314.
[7] J.T. Schriempf, A laser flash technique for determining thermal diffusivity of liquid metals at elevated temperatures, Rev. Sci. Instrum. 43 (1972) 781–786.
[8] Y. Nagasaka, T. Hatakeyama, M. Okuda, A. Nagashima, Measurement of the thermal diffusivity of liquids by the forced Rayleigh scattering method: theory and experiment, Rev. Sci. Instrum. 59 (1988) 1156–1168.
[9] J. Wang, M. Fiebig, Measurement of the thermal diffusivity of aqueous solutions of alcohols by a laser-induced thermal grating technique, Int. J. Thermophys. 16 (1995) 1353–1361.
[10] J.H. Kim, D. Chi, S.W. Kim, C.K. Choi, C. Rhee, The effects of grating period and heating duration time on the measurement of thermal diffusivity of liquids using photothermal gating spectroscopy, Measurement 15 (1995) 159–164.
[11] R.T. Bailey, F.R. Cruickshank, D. Pugh, S. Guthrie, A. McLeod, W.S. Foulds, W.R. Lee, S. Venkatesh, The determination of thermal conductivity coefficients of liquids by a thermal lens technique, Chem. Phys. 77 (1983) 243–246.
[12] V. Vilimpoc, T. Chen, R. Cole, P.C. Sukanek, A method for determining the thermal diffusivity of fluids, Int. J. Heat Mass Transfer 32 (1989) 778–780.
[13] S.C. Kim, T.F. Irvine Jr, A transient technique to determine the thermophysical properties of liquids, in: Proceedings of the Second World Conference on Experimental Heat Transfer, Fluid Mechanics and Thermodynamics, Dubrovnik, Yugoslavia, Elsevier, 1991, pp. 1546–1553.
[14] A.C. Boccara, D. Fournier, J. Badoz, Thermooptical spectroscopy-detection by the mirage effect, Appl. Phys. Lett. 36 (1980) 130–132.
[15] A. Salazar, A. Sanchez-Lavega, J. Fernandez, Theory of thermal diffusivity determination by the 'mirage' technique in solids, J. Appl. Phys. 65 (1989) 4150–4156.
[16] M. Bertolotti, G. Liakhou, R. Li Voti, F. Michelotti, C. Sibilia, Method for thermal diffusivity measurements based on photothermal deflection, J. Appl. Phys. 74 (1993) 7078–7084.
[17] S.I. Yun, K.D. Oh, K.S. Ryu, C.G. Kim, H.L. Park, H.J. Seo, C. Kum, Photothermal probe beam deflection measurement of thermal diffusivity of atmospheric air, Appl. Phys. B 40 (1986) 95–98.
[18] J. Sun, J.P. Longtin, T.F. Irvine Jr., Laser-based measurement of liquid thermal conductivity and thermal diffusivity, Proceedings of the 33rd National Heat Transfer Conference, NHTC99-266, Albuquerque, New Mexico, 1999.
[19] T. Kallard, Exploring Laser Light, Reprinted by American Association of Physics Teachers, 1982, pp. 202–203.
[20] J.D. Spear, R.E. Russo, R.J. Silva, Collinear photothermal deflection spectroscopy with light-scattering samples, Appl. Opt. 29 (1990) 4225–4234.
[21] H.S. Carslaw, J.C. Jaeger, in: Conduction of Heat in Solids, second ed., Oxford University Press, 1959, p. 347.
[22] J. Sun, Laser-based thermal pulse measurement of liquid thermal conductivity and thermal diffusivity, Master Thesis, State University of New York, Stony Brook, NY, 1999.
[23] D.R. Lide, in: D.R. Lide (Ed.), CRC Handbook of Chemistry and Physics, CRC Press, Boca Raton, FL, 1998.

[24] C.L. Yaws, Handbook of Transport Property Data, Houston Gulf Pub. Co, 1995.
[25] Y.S. Touloukian, Thermophysical Properties of Matter, the TPRC Data Series, A Comprehensive Compilation of Data, vol. 3 (1970), Vol. 10 (1973), IFI/Plenum, New York.
[26] C.F. Beaton, G.F. Hewitt, Physical Property Data for the Design Engineer, Hemisphere Publishing Co, Washington, 1988.
[27] K. Raznjevic, Handbook of Thermodynamic Tables and Charts, Hemisphere Pub. Co, Washington, 1976.
[28] N.B. Vargaftik, Tables on the Thermophysical Properties of Liquids and Gases, Hemisphere Pub. Co, Washington, 1975.
[29] J. Timmermans, Physico-chemical Constants of Pure Organic Compounds, Elsevier, New York, 1950.
[30] D. Solimini, Loss measurement of organic materials at 6328 Å, J. Appl. Phys. 37 (1966) 3314–3315.
[31] M.E. Lusty, M.H. Dunn, Refractive indices and thermo-optical properties of dye laser solvents, Appl. Phys. B 44 (1987) 193–198.